Microwave activation of electrochemical processes: convection, thermal gradients and hot spot formation at the electrode | solution interface

Frank Marken,* Yu-Chen Tsai, Barry A. Coles, Steven L. Matthews and Richard G. Compton

Physical and Theoretical Chemistry Laboratory, Oxford University, Oxford, UK OX1 3QZ.
E-mail: Frank.Marken@chemistry.oxford.ac.uk

Received (in Cambridge, UK) 20th April 2000, Accepted 21st July 2000
Published on the Web 15th August 2000

Microwave activation of electrochemical processes is possible by self-focussing of intense microwave radiation at the electrode | solution (electrolyte) interface of an electrode immersed in a solution and placed in a microwave cavity. Considerable changes in voltammetric current responses are observed experimentally for the one-electron reduction of $Ru(NH_3)_6^{3+}$ in aqueous 0.1 M KCl and for the stepwise two-electron reduction of the methylviologen dication (MV^{2+}) in aqueous 0.1 M NaCl. The formation and interconversion of two distinct forms of solid deposits, MV^0_{am} and MV^0_{cryst}, on a mercury electrode surface is investigated, both in the presence of microwave activation and with conventional heating. It is shown that microwave activation achieves (i) high temperatures in the vicinity of the electrode, (ii) thermal desorption of deposits from the electrode surface and (iii) limiting currents an order of magnitude higher compared to those induced by conventional isothermal heating to the same electrode temperature.

A simple physical model based on Joule heating of the aqueous solution phase is employed in a finite element simulation (FIDAP™) procedure to explain the differences observed experimentally between conventional heating and microwave activation. Based on the comparison of simulation and experimental data, a considerable thermal gradient and 'hot spot' region in the diffusion layer of the electrode, together with convective mass transport are proposed.

1 Introduction

Microwave activation of electrochemical processes has recently been shown to allow rapid heat pulses[1,2] or stable high temperature conditions[3] to be applied locally at the working electrode | solution (electrolyte) interface in electrochemical systems. The discovery of microwave activation as a novel tool in chemistry,[4,5] most notably in catalysis[6] and in organic synthesis,[7] has triggered interest in the effects of intense microwave radiation at interfaces.[8] Electrochemical measurements may offer a new approach for quantitative mechanistic studies at interfaces in the presence of intense microwave radiation. By coupling microwave radiation as a source of energy into the chemical process at the electrode surface, new types of processes, benefits and applications may result. Other methods of employing sources of energy for the enhancement or better control of electrochemical processes comprise, for example, photo-activation,[9] laser activation,[10] sonication,[11] radio-frequency heating,[12] as well as tribochemical[13] activation. In particular, the recent work by Gründler and coworkers[14–18] has highlighted the importance of thermal activation in electrochemistry.

Self-focussing of intense microwave radiation into the zone in front of a working electrode immersed in a liquid has been shown to have a considerable effect on the electrochemical process, to affect only processes in the vicinity of the electrode and to occur on a time scale fast enough for fast transient perturbation at small electrodes.[1] Details of the effect of microwaves on processes such as the formation of deposits, nucleation of conducting or non-conducting materials at the electrode | solution interface, or homogeneous chemical processes have yet to be explored. A physical model for the effect of microwaves at the electrode surface based on, *e.g.* a temperature profile induced by intense microwave radiation at the interface, and associated induced convection processes, requires development.

In this study, the use of microwave activation in electrochemical processes is investigated for the reduction of $Ru(NH_3)_6^{3+}$ as a model system of a 'simple' diffusion controlled process and the reduction of methylviologen dication (MV^{2+}) as a more complex system involving the formation of two distinct types of neutral deposits at the electrode surface. In particular, the differences between effects caused by conventional heating and by microwave activation are studied, and a physical model based on Joule heating is proposed to explain some of the effects induced by intense microwaves at electrode | solution (electrolyte) interfaces.

2 Experimental

2.1 Reagents

KCl, NaCl, HNO_3, $Hg(NO_3)_2$, $Ru(NH_3)_6Cl_3$ and methylviologen dichloride (all Aldrich) were obtained in the purest commercially available grade and used without further purification. Demineralised and filtered water with a resistivity of not less than 18 MΩ cm was taken from an Elgastat water purification system (Elga, Bucks, UK). Solutions were degassed using a vacuum system (*ca.* 15 Torr) or deareated with argon (Pureshield, BOC) for at least 15 min prior to undertaking experiments.

2.2 Instrumentation

For electrochemical experiments, a μ-Autolab II potentiostat system (Eco Chemie, Netherlands) was used. The electrochemical cell (see Fig. 1) consisted of a three electrode arrangement with a Pt-mesh counter electrode, a saturated

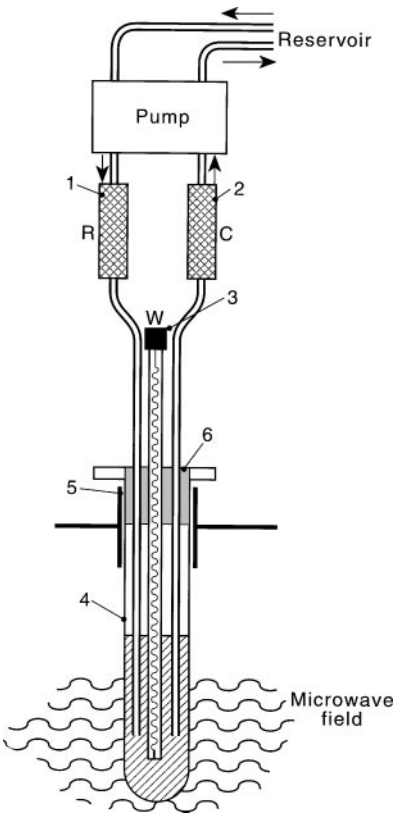

Fig. 1 Schematic drawing of the electrochemical cell used for *in situ* microwave activated voltammetry.

Calomel electrode (SCE) as reference, and a special microwave working electrode[3] with a 100 μm Pt disc sealed in glass (Micro Glass Instruments, Greensborough, Victoria, Australia or Scienglass, Long Hanborough, Oxfordshire, UK). For microwave activation experiments, a modified multi-mode microwave oven (Panasonic NN-3456, 2.45 GHz) with modified power supply, a water energy sink and a special port[19] for the electrochemical cell was used. Changing the anode current of the magnetron controlled the microwave intensity.

The design of the cell and microwave system is shown in Fig. 1. From a sample reservoir, solution is pumped *via* Teflon tubing through the reference electrode (1) and through a Teflon lid (6) into the electrochemical cell (4). The cell is inserted through a port (5) into a high intensity zone in the domestic microwave system. The working electrode (3) is located in the center of the cell. The fill height of the cell is kept constant by removal of solution past the counter electrode (2). The cell and electrode geometry have a considerable effect on the intensity of the microwave radiation focussed into the region close to the electrode surface. The effect of the cell fill height and electrode positioning were found to be crucial and optimized by maximizing the electrochemically detected limiting current increase.

Before operation, the system was tested for leaking microwave radiation with a radiation meter (Apollo XI microwave monitor, Apollo Ltd.). Experiments under conventional isothermal heating conditions were conducted in the same electrochemical cell immersed in a thermostatted bath.

For the deposition of a thin layer of mercury on the 100 μm diameter Pt disc electrode, the freshly polished electrode was immersed in a stirred solution of 10 mM Hg^{2+} in aqueous 0.1 M HNO_3. After five short deposition–stripping cycles (scan rate 0.1 V s^{-1}), mercury was deposited at $E = -0.1$ V *vs.* SCE for 2 min, giving a deposit corresponding to 70 μC charge or approximately 0.7 μm film thickness.[3]

Numerical simulations were carried out with a commercial finite element fluid dynamics software package, FIDAP™ (version 8.5), (Fluent Europe Ltd., Sheffield, UK, http://www.fluent.com) and executed on a Silicon Graphics Origin 2000. As the volume modelled (*vide infra*) is much smaller than the microwave wavelength, the microwave field was represented by a DC voltage boundary condition applied to the lower face of the solution volume, with a zero voltage boundary condition for the rear face of the glass rod and the platinum. A temperature boundary condition of 20 °C was applied to all the external faces. The solution was assigned a conductance of 10.0 S m^{-1} at 20 °C to simulate the loss component of the dielectric constant with a temperature dependence to simulate the temperature variation of the dielectric constant.[20] To allow for the penetration by the microwave field into the glass, this was assigned a conductance of 0.496 S m^{-1}, whose ratio to that of the solution was in the ratio of the dielectric constants of glass (3.84) and the solution (77.42). For the solution volume, FIDAP™ included a command to calculate the ohmic heating from the current flow induced by the applied voltage. No heating terms were included for the glass volume. The voltage boundary condition was then varied, as required, to give simulations yielding suitable electrode temperatures. To include convective flow, volume expansion data (for water) were entered for the solution, with the boundary conditions of zero gradient for velocity for the lower and the circumferential surfaces of the solution volume, zero velocity on the glass and platinum surfaces and zero radial velocity on the axis. The simulation was conducted in two stages with (i) the determination of the temperature distribution and convection effects followed by (ii) the simulation of faradaic currents due to electrochemical processes assuming a constant temperature distribution and convection. Effects due to the temperature dependence of the dielectric loss[4] and Soret diffusion, important, especially under extreme conditions, have not been accounted for. The finite element mesh (*vide infra*) and geometry have not been optimised. A possible error of $\geqslant 20\%$ for the quantitative prediction of limiting currents based on the simulation model has to be assumed at temperatures higher than 100 °C.

3 Results and discussion

3.1 The effect of microwaves on the reduction of $Ru(NH_3)_6^{3+}$

In Fig. 2, cyclic voltammograms for the reduction of 2 mM $Ru(NH_3)_6^{3+}$ in aqueous 0.1 M KCl (see eqn. 1) obtained with a 100 μm diameter Pt disc electrode and a scan rate of 0.1 V s^{-1} are shown.

$$Ru(NH_3)_6^{3+} + e^- \rightleftarrows Ru(NH_3)_6^{2+} \quad (1)$$

In Fig. 2a, the cyclic voltammogram obtained in the absence of microwave radiation is shown, and in Fig. 2b–d microwave radiation with increasing power is applied (see

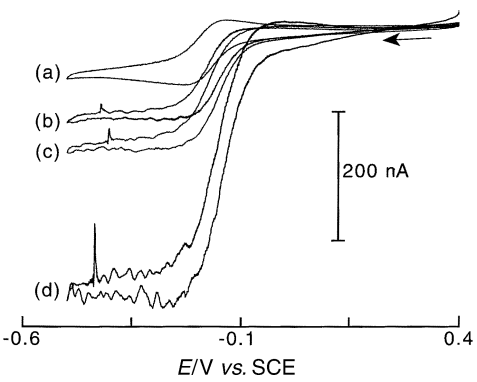

Fig. 2 Cyclic voltammograms for the reduction of 2 mM $Ru(NH_3)_6^{3+}$ in aqueous 0.1 M KCl at a 100 μm diameter Pt disc electrode with microwave power settings (magnetron anode current) of (a) 0, (b) 14, (c) 18 and (d) 20 mA (scan rate 100 mV s^{-1}).

Table 1 Halfwave potential data obtained from cyclic voltammograms for the reduction of 2 mM $Ru(NH_3)_6^{3+}$ in aqueous 0.1 M KCl at 20 ± 2 °C at a 100 μm diameter Pt disc electrode, without and with applied microwave radiation (scan rate 0.1 V s^{-1}, see Fig. 2)

Anode current, /mA	$E_{1/2}$ [a] /V *vs.* SCE	$T_{electrode}$ [b] /°C	I_{lim} [c] /nA
0	−0.181	20	−65
14	−0.172	40	−72
18	−0.168	48	−128
20	−0.162	61	−185
22	−0.151	85	−407
24	−0.166	53	−660

[a] Obtained from cyclic voltammograms by taking the mid-point of the currents from $\frac{1}{2}(I_{forward} + I_{backward})$ at each potential and determining the potential at $I = \frac{1}{2} I_{lim}$. [b] Temperature estimated from $E_{1/2}$ data by using $dE/dT = 0.46$ mV K^{-1}. [c] Limiting current observed in cyclic voltammogram.

Table 1). It can be observed that the shape of the voltammograms changes from peak-shaped in the absence of microwaves, characteristic for 'planar' diffusion controlled processes in stagnant solution, to sigmoidal at high microwave intensity, indicative of convergent diffusion or convection. The increase in current is accompanied by a concomitant shift in equilibrium potential. Therefore, the shift in half wave potential, $E_{1/2}$, for the electrochemically reversible voltammetric response (see Table 1) can be related to the average temperature at the electrode surface, $T_{electrode}$, if effects other than the reaction entropy for the half cell process[21] are assumed insignificant. The shift of the equilibrium potential has been determined recently in a uniformly heated electrochemical system[22] as 0.46 mV K^{-1}. Based on this thermal effect, the average temperature at the electrode surface during microwave activation was estimated (Table 1). Electrochemical reversibility of the voltammetric responses was ensured by confirming the Tomeš criterion,[23] $E_{3/4} - E_{1/4} = \ln 9 \times RT/F$, where $E_{3/4}$ and $E_{1/4}$ are the potentials at which the current reaches 3/4 or 1/4 of the limiting current, R is the gas constant, T is the absolute temperature, and F denotes the Faraday constant. It can be seen that the temperature at the electrode surface, $T_{electrode}$, increases with increasing microwave power. From the last entry in Table 1, it can be seen that, under more extreme conditions, an increase in current may be associated with an apparent decrease in temperature. It is possible that, depending on the degree of degassing of the solution phase, new effects may arise, for example due to bubble formation at elevated temperatures.

Analogous experiments with a 100 μm diameter Pt disc electrode and with a 100 μm diameter Pt electrode after coating with mercury were conducted. Consistent with results reported recently,[3] the effects of microwave radiation are essentially identical independent of the mercury coating at the electrode surface. Therefore, it may be concluded that for a simple diffusion controlled reversible electrode process, $Ru(NH_3)_6^{3+/2+}$, microwave activation causes (i) a thermal effect, detected *via* the shift in the reversible half wave potential, and (ii) a change in the shape of the voltammetric response from peaked to sigmoidal, associated with a considerable increase in current magnitude.

3.2 The effect of microwaves on the reduction of methylviologen

In aqueous media the methylviologen dication (MV^{2+}) is reduced in two consecutive and reversible one-electron processes (eqn. 2 and 3), with a more complex deposition process accompanying the second reduction step.[24–28]

$$MV^{2+}(aq) + e^- \rightleftarrows MV^+(aq) \quad (2)$$

$$MV^+(aq) + e^- \rightleftarrows MV(aq) \quad (3)$$

Both reduction products, $MV^+(aq)$ and $MV^0(aq)$ may undergo association processes in aqueous solution,[28] and at concentrations in excess of *ca.* 0.1 mM $MV^{2+}(aq)$, solid MV^0 is deposited on the electrode surface.[25] In Fig. 3a–d, cyclic voltammograms for the reduction of (a) 1 mM, (b) 2 mM, and (c) 4 mM MV^{2+} in aqueous 0.1 M NaCl obtained at a 100 μm diameter Pt–Hg electrode (see Experimental) are shown. The two one-electron reduction steps are observed at $E_{1/2}(MV^{2+/+}) = -0.69$ V and $E_{1/2}(MV^{+/0}) = -1.02$ V *vs.* SCE. During the course of the second reduction process two distinct types of deposit are detected, as identified by Evans and Engelman;[25] amorphous, MV^0_{am}, and crystalline, MV^0_{cryst}. In the initial stages of the deposition process, the amorphous deposit covers the entire electrode surface in the form of a thin layer.[24]

$$MV^0(aq) \rightleftarrows MV^0_{am}(s) \quad (4)$$

This deposit, MV^0_{am}, is detected *via* a stripping response on the reverse potential scan at *ca.* −1.0 V *vs.* SCE (see Fig. 3). Nucleation of the crystalline form, MV^0_{cryst}, occurs subsequently[24] and the crystalline material is detected in a new stripping response at approximately −0.9 V *vs.* SCE (eqn. 5).

$$MV^0_{am}(s) \rightleftarrows MV^0_{cryst}(s) \quad (5)$$

This solid–solid transformation has been shown to be initiated by a nucleation process and accompanied by morphological change in the deposit.[24] At low concentrations of $MV^{2+}(aq)$, and at elevated temperatures, the formation of MV^0_{cryst} is suppressed. In addition to the processes given in eqn. 2–5, there are likely to be numerous homogeneous and

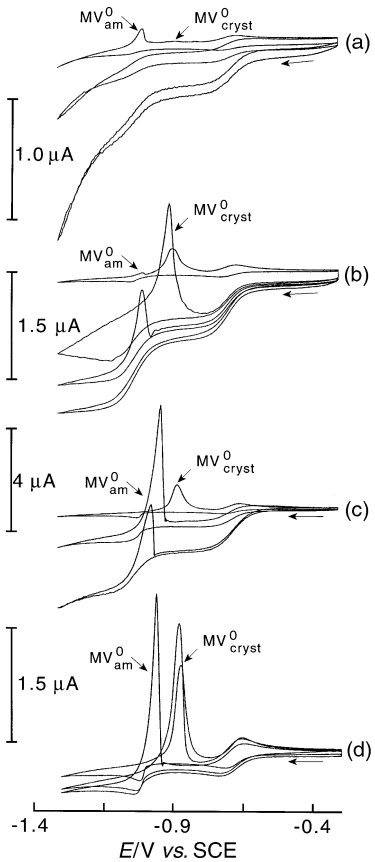

Fig. 3 Cyclic voltammograms for the reduction of (a) 1 mM MV^{2+}, (b) 2 mM MV^{2+}, (c) 4 mM MV^{2+} and (d) 4 mM MV^{2+} in aqueous 0.1 M NaCl obtained at a 100 μm diameter Pt–Hg electrode (scan rate 100 mV s^{-1}, anode currents (a) 0, 20, 22 mA, (b) 0, 20, 22, 23 mA, (c) 0, 20, 22 mA, (d) temperature 25, 54 and 64 °C).

heterogeneous cross-redox reaction steps which further complicate the process.

In Fig. 3a–c, it can be seen that, in the absence of thermal activation and with a scan rate of 0.1 V s^{-1}, MV^0_{am} is detected at a concentration of 1 mM MV^{2+}, but MV^0_{cryst} dominates the deposition process at the higher concentration of 4 mM MV^{2+}. The application of focussed microwave radiation causes a considerable change in the appearance of the voltammetric responses. The stripping response for MV^0_{cryst} initially increases until, at higher microwave power, a switch to the stripping response associated with MV^0_{am} occurs. Finally, both stripping responses vanish and the overall process shows no sign of a deposition process. That is, microwave activation can be employed to keep the electrode surface active and free of deposit (see Fig. 3b). A similar trend is observed when conventional thermal activation of the electrode process is applied.[24] In Fig. 3d, cyclic voltammograms for the reduction of 4 mM MV^{2+} at a 100 μm diameter Pt–Hg electrode at elevated temperatures are shown. An increase of the stripping response at elevated temperature and a characteristic 'switch' from MV^0_{cryst} to MV^0_{am} can be observed at *ca.* 60 °C. Comparison of the temperatures at which the 'switch' occurs between thermal (*ca.* 60 °C) and microwave activated systems (20 mA magnetron anode current consistent with *ca.* 61 °C, see Table 1) suggests that, in both cases, very similar processes occur. However, the formation of the crystalline deposit, MV^0_{cryst}, requires nucleation and is not an equilibrium process, therefore, effects from concentration and convection may further affect the solid–solid transformation and complicate the comparison of results.

Although the effect of the temperature increase on the stripping responses for MV^0 with conventional heating follows the same trend compared to that observed with microwave activation, there are considerable differences in the limiting currents detected (see Fig. 3c and d). Microwave activation causes limiting currents an order of magnitude higher compared to those observed during measurements with isothermal heating. It is very likely that the thermal gradients induced by non-isothermal heating are responsible for the onset of convection processes, which further increase the mass transport towards the electrode surface and, therefore, cause higher currents. In order to further study the effect and the nature of thermal gradients induced by focussed microwave radiation at the electrode surface, a finite element simulation procedure based on a simple physical model has been employed.

3.3 A FIDAP™ model of the effect of microwaves on electrochemical processes

Heat dissipation, convection, and thermal gradients at the electrode surface in a microwave activated electrochemical system can be modelled by a FIDAP™ finite element simulation. Microwave heating occurs in media with dielectric loss,[4] such as polar liquids or electrolyte solution. Therefore, thermal activation will occur predominantly in the solution phase. In the simulation, Joule heating of the solution phase (Fig. 4a) is applied *via* a potential between the lower boundary and the metal electrode. The thermal conductivity for glass, water, and platinum, as well as density and viscosity data for an aqueous solution of 0.1 M KCl (see Table 2) have been used as input parameters. The model comprised a 0.1 cm length of glass rod of 0.1 cm radius, containing a 100 μm diameter platinum wire at its centre, with a flat face to form the microdisc electrode, in contact with a cylindrical volume of solution of 0.1 cm radius and 0.15 cm long (Fig. 4a). The simulation was performed (see Experimental) in an axisymmetric mode on a two-dimensional radial section of this model. A finite element mesh was employed with a fine mesh (0.8 μm) close to the electrode surface and expanding in the regions of low gradients.

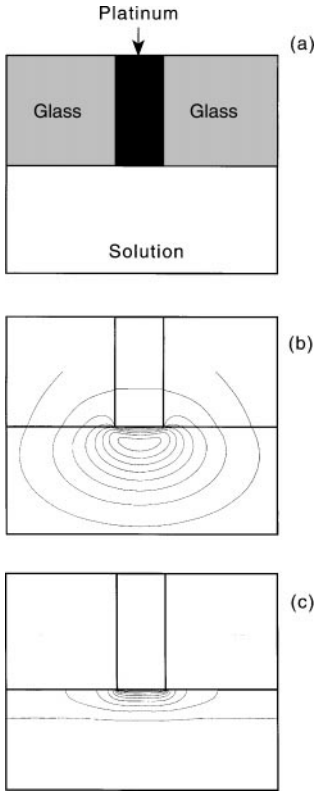

Fig. 4 (a) Schematic drawing of the model applied in the finite element (FIDAP™) simulation procedure for a 100 μm diameter platinum electrode. (b) Contour plot of the thermal gradient developed with $T_{electrode} = 86$ °C and $T_{hot\ spot} = 191$ °C (contour lines = 63, 80, 97, 114, 131, 149, 165 and 183 °C). (c) Contour plot for the concentration gradient developed for the mass transport controlled reduction of $Ru(NH_3)_6^{3+}$ with $T_{electrode} = 86$ °C (contour lines = 5, 15, 25, 35, 45, 55, 65, 75, 85, and 95% of bulk concentration).

The thermal effect calculated in the simulation is most pronounced close to the electrode surface, where the current density is high (focussing). However, the ability of platinum to conduct heat more efficiently than water introduces a thermal gradient adjacent to the electrode surface and within the diffusion layer of the electrode. The temperature contours shown in Fig. 4b correspond to the case of an electrode temperature of 86 °C and a 'hot spot' temperature of 191 °C. The difference between the temperature at the electrode surface, $T_{electrode}$,

Table 2 Data used for the numerical simulation (FIDAP™) of diffusion and convective flow processes at a Joule-heated electrochemical system (see Fig. 4)

Parameter	Comments	Reference
Diffusion coefficients	Based on $D(T) = D_{293} \times \exp \frac{E_A}{R}\left(\frac{1}{293} - \frac{1}{T}\right)$	12
	$Ru(NH_3)_6^{3+}$ in 0.1 M KCl: $D_{293} = 6.17 \times 10^{-6}$ cm^2 s^{-1}, $E_A = 22\,500$ J mol^{-1}	
Viscosity	For water; taken from published data	29
Specific heat	For water; taken from published data	30
Thermal conductivity	For water; taken from published data	30

and the temperature in the 'hot spot' region, $T_{\text{hot spot}}$, under these conditions is considerable and plotted in Fig. 5a. It can be seen that, in the solution phase, temperatures much more extreme than at the electrode surface are possible and the problem of bubble nucleation and boiling at the solid | liquid interface can therefore be avoided. Very similar effects of 'inverted heat transfer' and 'super heating' have been postulated for the effects observed during microwave heating of chemical reactions.[31] For electrochemical processes, the presence of a thermal gradient and 'hot spot' near the electrode surface is unique and may be regarded as a key to novel applications.

In Fig. 5b a plot of the limiting current for the reduction of $Ru(NH_3)_6^{3+}$ at a 100 μm diameter electrode as a function of $T_{\text{electrode}}$, calculated based on the temperature dependence of the diffusion coefficient of $Ru(NH_3)_6^{3+}$(aq) (see Table 2), is shown. Here, two simulation models are compared, in which (i) a stagnant solution and (ii) a thermally driven convection process are considered. The increase in the limiting current in the absence of convection, governed only by the temperature effect on diffusion, is moderate. When convection is considered in the model, a gravity driven flow of liquid is induced with a maximum velocity at a distance of 15 μm from the centre of the electrode surface of 1.4 mm s^{-1} towards the electrode surface. The resulting increase in the limiting current is shown in Fig. 5b, together with experimental data obtained for the reduction of 1 mM $Ru(NH_3)_6^{3+}$ at a 100 μm diameter platinum electrode. The approximate agreement of experimental and simulation limiting current data suggests a considerable contribution from convection and therefore lends credibility to the simple physical model, at least for the case of 'moderate' applied microwave power.

The concentration contours in the case of the mass transport controlled reduction of $Ru(NH_3)_6^{3+}$ at the 100 μm diameter platinum electrode are shown in Fig. 4c. The outermost line of the concentration profile corresponds to 95% bulk concentration and may be considered as a measure of the diffusion layer thickness in the presence of Joule heating and with $T_{\text{electrode}} = 86\,°C$. Due to the convection process, the diffusion layer is compressed towards the electrode surface. Perhaps surprisingly, the hot spot region is located *within* the diffusion layer. Therefore, molecules diffusing into the hot spot region are also very likely to undergo electron transfer at the electrode surface. An order of magnitude estimate of the approximate time between transit through the hot zone and reaction at the electrode surface may be obtained as $\Delta t \approx [\Delta x^2/D(T)] \approx 20$ ms.

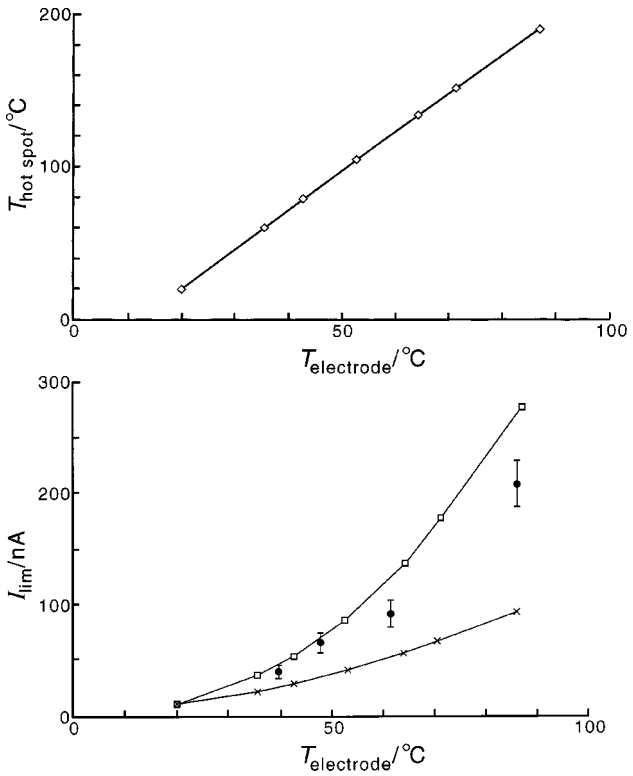

Fig. 5 (a) Plot of the simulation result for the temperature at the electrode surface, $T_{\text{electrode}}$, *vs.* the hot spot temperature, $T_{\text{hot spot}}$, for the case of Joule heating with convection. (b) Plot of the mass transport controlled limiting currents simulated for the reduction of 1 mM $Ru(NH_3)_6^{3+}$ at a 100 μm diameter disc electrode without (×) and with convection (□) processes. Also shown are experimental data points for the reduction of $Ru(NH_3)_6^{3+}$.

4 Conclusions

It has been shown that microwave activation of electrochemical processes allows (i) the temperature at the electrode surface to be increased, (ii) a thermal gradient and a 'hot spot' zone within the diffusion layer to be achieved, and (iii) a convective flow to be induced. Both thermal activation and higher mass transport are beneficial for electrochemical applications. For the complex methylviologen reduction process involving the formation of a solid product and a solid–solid transformation, microwave activation does not qualitatively change the reaction pathway or introduce novel effects. However, from the differences observed in voltammetric experiments under microwave radiation and with conventional heating, the advantages of microwave activation are obvious. Further quantitative studies of the effect of intense microwave radiation on the rate constant and pathway of a chemical process will have to take into consideration the thermal gradient induced by microwave radiation at the electrode surface | solution interface.

Acknowledgements

S. M. gratefully acknowledges support from the Nuffield Foundation (Summer Studentship AT/100/99/0019) and from New College, Oxford. F. M. thanks the Royal Society for the award of a University Research Fellowship and New College for a Stipendiary Lectureship. This work was undertaken as part of the EU sponsored D10 COST Programme (Innovative Methods and Techniques for Chemical Transformations).

References

1 R. G. Compton, B. A. Coles and F. Marken, *Chem. Commun.*, 1998, 2595.
2 R. P. Akkermans, S. L. Roberts, F. Marken, B. A. Coles, S. J. Wilkins, J. A. Cooper, K. E. Woodhouse and R. G. Compton, *J. Phys. Chem. B*, 1999, **103**, 9987.
3 F. Marken, S. L. Matthews, R. G. Compton and B. A. Coles, *Electroanalysis*, 2000, **12**, 267.
4 For a review, see: C. Gabriel, S. Gabriel, E. H. Grant, B. S. J. Halstead and D. M. P. Mingos, *Chem. Soc. Rev.*, 1998, **27**, 213.
5 *Microwave-Enhanced Chemistry*, eds. H. M. Kingston and S. J. Haswell, American Chemical Society, Washington, 1997.
6 See, for example: J. R. Thomas, *Catal. Lett.*, 1997, **49**, 137.
7 For a review, see: F. Langa, P. De La Cruz, A. De La Hoz, A. Diaz-Ortiz and E. Diez-Barra, *Contemp. Org. Synth.*, 1997, 373.
8 (*a*) S. J. Haswell and N. Howarth, *Anal. Chim. Acta*, 1999, **387**, 113; (*b*) R. Maoz, H. Cohen and J. Sagiv, *Langmuir*, 1998, **14**, 5988.
9 R. G. Compton and R. A. W. Dryfe, *Prog. React. Kinet.*, 1995, **20**, 245.
10 R. P. Akkermans, M. F. Suarez, S. L. Roberts, F. L. Qiu and R. G. Compton, *Electroanalysis*, 1999, **11**, 1191.
11 A. J. Saterlay, C. Agra-Gutiérrez, M. P. Taylor, F. Marken and R. G. Compton, *Electroanalysis*, 1999, **11**, 1083.
12 F. Qiu, R. G. Compton, B. A. Coles and F. Marken, *J. Electroanal. Chem.*, in press.
13 V. I. Varentsova, V. K. Varentsov and V. V. Boldyrev, *J. Appl. Chem. (USSR)*, 1990, **63**, 531.
14 P. Gründler and A. Kirbs, *Electroanalysis*, 1999, **11**, 223.

15 T. Zerihun and P. Gründler, *J. Electroanal. Chem.*, 1998, **441**, 57.
16 T. Zerihun and P. Gründler, *J. Electroanal. Chem.*, 1996, **404**, 243.
17 A. Beckmann, B. A. Coles, R. G. Compton, P. Gründler, F. Marken and A. Neudeck, *J. Phys. Chem. B*, 2000, **104**, 764.
18 M. Jasinski, A. Kirbs, M. Schmehl and P. Gründler, *Electrochem. Commun.*, 1999, **1**, 26.
19 D. M. P. Mingos and D. R. Baghurst, *Microwave-Enhanced Chemistry*, ed. H. M. Kingston and S. J. Haswell, American Chemical Society, Washington, 1997, ch. 1.
20 A. C. Metaxas, *Foundations of Electroheat*, Wiley, New York, 1996.
21 See, for example: J. W. Turner and F. A. Schulz, *Inorg. Chem.*, 1999, **38**, 358 and references cited therein.
22 R. Akkermmans, M. Suarez, S. Roberts, Q. Fulian and R. G. Compton, *Electroanalysis*, 1999, **11**, 1191.
23 K. B. Oldham and J. C. Myland, *Fundamentals of Electrochemical Science*, Academic Press, New York, 1994, p. 217.
24 F. Qiu, R. G. Compton, F. Marken, S. J. Wilkins, C. H. Goeting and J. S. Foord, *Anal. Chem.*, 2000, **72**, 2362.
25 E. E. Engelman and D. H. Evans, *Langmuir*, 1992, **8**, 1637.
26 E. E. Engelman and D. H. Evans, *J. Electroanal. Chem.*, 1993, **349**, 141.
27 A. E. Kaifer and A. J. Bard, *J. Phys. Chem.*, 1985, **89**, 4876.
28 M. Rueda, R. G. Compton, J. A. Alden and F. Prieto, *J. Electroanal. Chem.*, 1998, **443**, 227.
29 V. M. M. Lobo, *Handbook of Electrolyte Solutions*, Elsevier, Amsterdam, 1989.
30 *CRC Handbook of Chemistry and Physics*, 74th edn., CRC Press, London, 1994.
31 D. R. Baghurst and D. M. P. Mingos, *Chem. Commun.*, 1992, 674.